THE JOURNAL OF PHYSICAL CHEMISTRY B

ARTICLE

pubs.acs.org/JPCB

Conformational Heterogeneity within the Michaelis Complex of Lactate Dehydrogenase

Hua Deng,*[,†] Dung V. Vu,[‡] Keith Clinch,[§] Ruel Desamero,[∥] R. Brian Dyer,[⊥] and Robert Callender[†]

[†]Department of Biochemistry, Albert Einstein College of Medicine, Bronx, New York 10461, United States

[‡]Bioscience Division, Los Alamos National Laboratory, Los Alamos, New Mexico 87545, United States

[§]Industrial Research Ltd., P.O. Box 31-310, Lower Hutt. 5040, New Zealand

[∥]Department of Chemistry, York College, CUNY, Jamaica, New York 11451, United States

[⊥]Department of Chemistry, Emory University, Atlanta, Georgia 30322, United States

ABSTRACT: A series of isotope edited IR measurements, both static as well as temperature jump relaxation spectroscopy, are performed on lactate dehydrogenase (LDH) to determine the ensemble of structures available to its Michaelis complex. There clearly has been a substantial reduction in the number of states available to the pyruvate substrate (as modeled by the substrate mimic, oxamate) and NADH when bound to protein compared to dissolved in solution, as determined by the bandwidths and positions of the critical C_2═O band of the bound substrate mimic and the C_4−H stretch of the NADH reduced nicotinamide group. Moreover, it is found that a strong ionic bond (characterized by a signature IR band discovered in this study) is formed between the carboxyl group of bound pyruvate with (presumably) Arg171, forming a strong "anchor" within the protein matrix. However, conformational heterogeneity within the Michaelis complex is found that has an impact on both catalytic efficiency and thermodynamics of the enzyme.

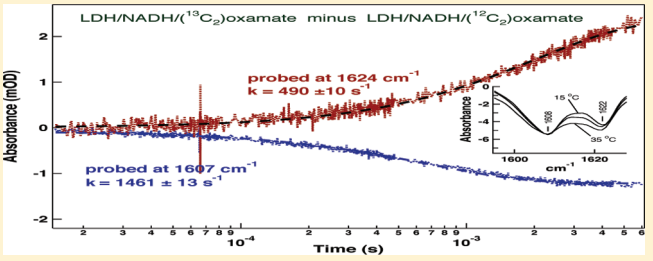

It has long been recognized that a protein does not occupy a unique folded single three-dimensional array of atoms as might be supposed from X-ray structures. Rather, the protein's structure is described as occupying a hierarchy or ensemble of interconverting conformations on multiple time scales and spatial extent.[1−4] This physics has generally been neglected within the usual and simplistic notions of the nature of the Michaelis complex in enzymatic catalysis. Generally for single step reactions, the textbooks have it that there is a single conformation of the enzyme/substrate complex that is poised to cross over the transition state barrier to form enzyme/product. In contradiction to this view, the central issue that this work addresses is whether or not an enzyme Michaelis complex exists in multiple conformations. That is, how is the ensemble of structures available to the enzyme/substrate complex distributed and are some conformations further along the reactive pathway than others ("closer" toward the transition state). Answers to these questions are important to obtain concerning (1) on what time scales and dynamical paths does the system "arrive" at the chemical event and (2) how are the thermodynamic parameters normally determined for enzyme systems (for example, the activation enthalpy of the reaction) related to this more complicated, but more physical, view of the dynamics of the enzyme/substrate system. A more thorough discussion of these issues is provided in refs 5 and 6 Here, we carry out a series of isotope edited IR measurements on the enzyme lactate dehydrogenase (LDH) to characterize catalytically relevant conformations of a faithful mimic of its Michaelis complex.

LDH, normally existing as a 140 kDa tetramer, catalyzes the conversion between pyruvate and lactate, using NADH/NAD^+ as cofactor. This enzyme has been studied extensively by X-ray crystallography, and a number of structures of LDH from various sources complexed with cofactor NADH and a pyruvate analog, oxamate, have been published (cf., for the isozyme employed in this study, *Bacillus stearothermophilus* (bsLDH), refs 7 and 8). The active site contacts so revealed identified several important hydrogen bonds to the substrate analog, oxamate. The C_2═O bond of oxamate forms hydrogen bonds with His195 and Arg109, and both of them are likely positively charged.[9] The C_1 carboxyl group of oxamate forms a guanidinium−carboxylate salt bridge, which involves the active site Arg171 (Scheme 1).

Theoretical calculations[10−12] and experimental work[13] have suggested that the features of the transition state structure of the hydride transfer reaction include a ring puckering of the dihydronicotinamide of NADH, which renders the transferred hydrogen at the pseudoaxial position. It has been demonstrated[14] that the polarization of the pyruvate C_2═O bond of bound pyruvate is strongly and quantitatively correlated to catalytic

Received: February 17, 2011
Revised: April 15, 2011
Published: May 13, 2011

ACS Publications © 2011 American Chemical Society

Scheme 1. The Active Site Contacts of Pyruvate and NADH Bound to LDH with Key Residues As Determined by X-ray Crystallography[a]

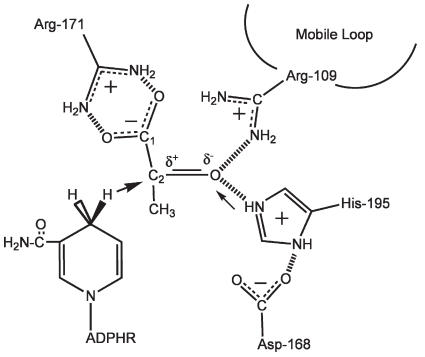

[a] The reaction catalyzed by LDH involves the direct transfer of a hydride ion from C4 of the reduced nicotinamide group of NADH to the C2 carbon of pyruvate accompanied by the protonation of pyruvate's keto oxygen, the proton being supplied by His195 (the arrows in the diagram indicate the H^- and H^+ transfers). It is known that either electrostatic stabilization of the transition state in the pyruvate−lactate interconversion, which contains a highly polarized carbonyl moiety, $^+C-O^-$, or destabilization of the >C═O ground state (or a combination) is responsible for about half of the rate enhancement brought about by LDH. The other half of the rate enhancement comes about from bringing cofactor and substrate close together in a proper orientation and "activating" cofactor towards catalysis. The substrate mimic used here, oxamate, differs from pyruvate by the replacement of the $-CH_3$ group to an $-NH_2$ moiety.

efficacy:

$$k_{\text{hydride}}(s^{-1}) = \exp^{0.21(\Delta\nu_{C=O})} + 0.0042 \qquad (1)$$

where the stretching frequency of the C_2═O bond is a direct measure of bond polarization. The structural changes and electrostatic interactions of active site charged contacts between the substrate's C_2═O bond with His195 and Arg109 contribute as much as 6 orders of magnitude reaction rate acceleration of the LDH catalysis, out of the total 10^{14} rate enhancement.

Isotope edited difference FTIR techniques (cf. refs 15 and 16) determine the frequencies of key bonds within the LDH/NADH/oxamate complex, including the C_2═O and antisymmetyric carboxylate, $-C_1OO^-$, stretch modes of the bound substrate mimic. Several questions are to be investigated in this study. Some are technical. We present here details of our subtraction procedures sufficient for others to reproduce our results and carry out other studies. Isotope editing of vibrational spectra (either Raman[17] or IR) of proteins removes background spectrum of many overlapping bands to yield spectra assigned to specific vibrational modes. However, very sensitive subtractions are made at the level of 0.1%, and errors of various types must be assessed. In the course of these studies, we also measured a heretofore not observed vibrational mode that involves motions of the guanidinium−carboxylate salt bridge discussed above. The guanidinium−carboxylate salt bridge is important in the catalytic mechanism of many enzyme systems and in the structural integrity of many proteins. Identification of this salt bridge in proteins normally requires a high resolution structure of the entire protein, although other spectroscopy methods have been applied to small protein systems[18] or indirectly infer its existence and properties.[19] But the main question concerns an elucidation of the ensemble of structures of the Michaelis complex of LDH.

MATERIALS AND METHODS

NADH and oxamate were purchased from Roche. ^{15}N-labeled ammonium chloride was purchased from Cambridge Isotope Lab. $^{13}C_2$ labeled oxamate was made according to a published procedure.[20] The synthesis of $^{13}C_1$-labeled oxamate is described in ref 21.

The bsLDH gene was obtained from genomic DNA from *Geobacillus stearothermophilus* ATCC 12980D and subcloned to pET3a vector from New England Biolabs using restriction enzymes Nde1 and BamH1 and standard molecular biology procedures. The integrity of the gene was verified by sequencing. The plasmids were transformed into C43(DE3) competent *Escherichia coli* cells from OverExpress for LDH expression. The growth conditions of the cells and the purification procedures were otherwise the same as those published previously.[14] The purity was estimated to be >95% using sodium dodecyl sulfate (SDS) gels. ^{15}N uniformly labeled bsLDH was obtained by growing the C43-(DE3) cells at 37 °C in minimal media supplemented with 1 g of ^{15}N-labeled ammonium chloride and 10 g of glucose per liter of culture media. The expression of bsLDH was induced by the addition of isopropyl-β-D-thiogalactopyranoside (IPTG) to the culture media to a final concentration of 0.5 mM when the cell density reached 0.8 to 1.2 OD at 600 nm. After 15 h, the cells were harvested, and the ^{15}N uniformly labeled bsLDH was purified according to the same procedure as the unlabeled bsLDH. Pig heart LDH (phLDH) was purchased from Roche Diagnostics (Indianapolis, IN) and prepared as previously described.[22]

Static Isotope-Edited Fourier Transform Infrared (FTIR) Difference Spectroscopy. This was performed using a Magna 760 Fourier transform spectrometer (Nicolet Instrument Corp., WI) outfitted with a mercury−cadmium−telluride (MCT) detector. A two-position sample shuttle controls alternation between the labeled and unlabeled sample positions. IR cells consisted of CaF_2 windows with 15-μm Teflon spacers. Spectra were collected in the range of 1100−4000 cm^{-1} with 2 cm^{-1} resolution. A Blackman−Harris three-term apodization and a Happ−Genzel apodization were applied, respectively. Omnic 4.1a (Nicolet Instruments, Corp.) software was used for data collection and analysis. All samples were prepared in D_2O buffer with 50 mM triethanolamine, 5 mM fructose 1,6-bis phosphate, and 150 mM NaCl at pH7.4 (pH meter reading); measurements were conducted at 295 K. The concentrations for LDH:NADH:oxamate were, approximately, 4:4:4 mM (where LDH concentration refers to active sites). Typically, 128 scans were collected for each sample.

The difference spectroscopy was performed in a systematic way. First, concentrated NADH (~100 mM) was added to a LDH sample (~5 mM active sites), and then the binary complex sample was divided into two parts. This reduces the possibility of having different NADH concentration in the ternary complexes. The stock solutions of isotope-labeled and unlabeled oxamate concentrations (~100 mM) were estimated by their characteristic IR band intensities, and appropriate quantities were added to the separate LDH/NADH complexes to make the two samples for the initial isotope-edited difference FTIR experiment. Since the estimated concentrations of the oxamate solutions are not precisely accurate (typically within ~2% of each other), the first isotope-edited difference FTIR spectrum inevitably contains extra protein bands due to the imbalance of the bound oxamate and/or NADH in the two samples. The difference spectra between LDH/NADH and LDH and between LDH/NADH/oxamate

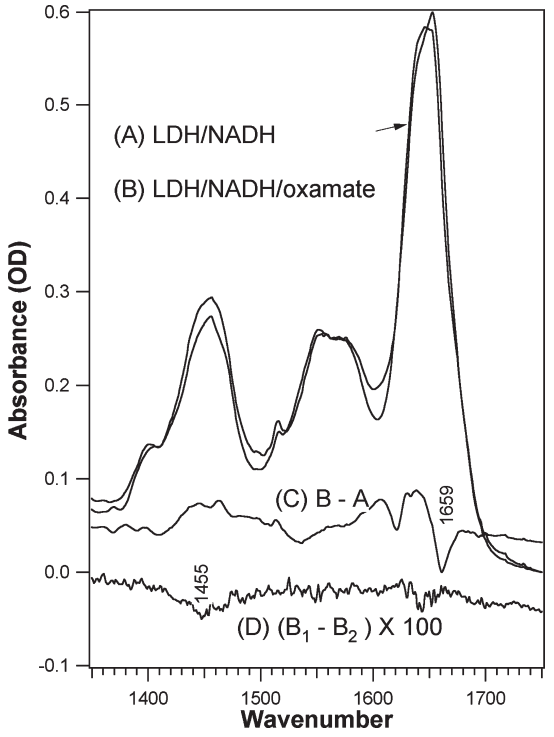

Figure 1. The FTIR spectra of (A) LDH/NADH complex; (B) LDH/NADH/oxamate complex; (C) difference between spectra b and a, and (D) difference between two LDH/NADH/oxamate complexes prepared identically. The intensity for spectrum d is multiplied by a factor of 100. All samples were prepared in D_2O buffer with 50 mM triethanolamine, 5 mM fructose 1,6-bis phosphate, and 150 mM NaCl at pH7.4 (pH meter reading); the measurements were conducted at 295 K. The concentrations for LDH:NADH:oxamate were 4:4:4 mM. All solvent bands were subtracted from the presented spectra.

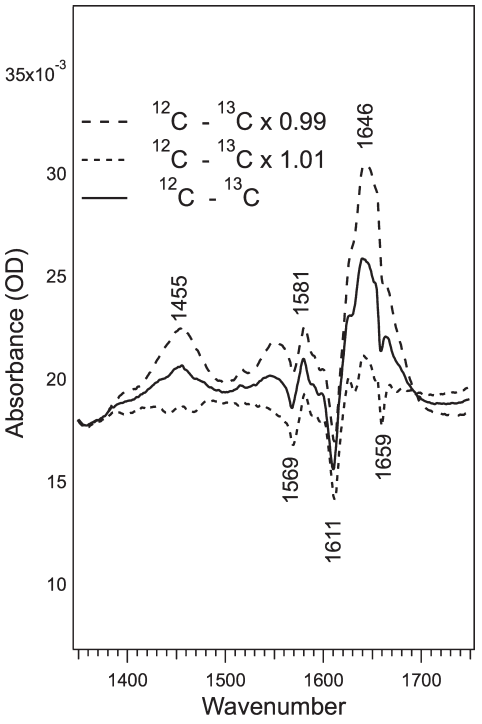

Figure 2. The difference FTIR spectra between LDH/NADH/[$^{12}C_1$]oxamate complex with and [$^{13}C_1$]oxamate using three different subtraction factors. Top curve: subtraction factor 0.99; middle curve: 1.00; and bottom curve: 1.01. Experimental conditions are given in Figure 1.

and LDH/NADH were then obtained to identify the possible marker bands that would indicate an imbalance in the two samples used for the isotope-edited difference measurements. For example, if a negative band at 1659 cm^{-1} appeared in the isotope edited difference spectrum, it was likely that the oxamate concentration in the ternary complex with the unlabeled oxamate was higher (according to spectrum Figure 1C). Thus, in the next iteration, the amount of oxamate added to LDH/NADH could be adjusted accordingly. Since the appearance of these protein bands can result from a number of factors relating to an imbalance between the two samples, such as a small difference in oxamate and/or NADH concentrations, a small difference in the hydrogen concentration in deuterated samples, small temperature variations in the two samples, and even equilibrium binding isotope effects, typically about 10 iterations are required before a relatively clean isotope-edited difference spectrum can be obtained to allow the assignments of vibrational modes associated with bound oxamate. These assignments can be made even in the presence of protein "artifacts". The reported frequencies for most of the IR bands are based on the average of more than five separate measurements with an error of ± 1 cm^{-1}. The uncertainties for certain broad bands are larger and are reported when needed.

Although isotope-edited difference FTIR measurements have been applied to enzyme systems before (e.g., ref 23), assignments of weak bands are still difficult due to unbalanced protein/ligand concentration ratios of the isotope-labeled and unlabeled samples. Thus, we used a special procedure to ensure that the sample mismatch does not lead to false band assignments as described in the Results. Corrections in the resulting difference spectrum have been made for (1) HOD, which shows a relatively broad marker band near 1455 cm^{-1} and (2) for the subtraction of unbalanced water vapor, which has many sharp bands in the spectral region of interest. Both these can contribute bands in a difference spectrum since the contributions from HOD and water vapor are typically slightly unbalanced between the two samples. However, these subtract well, and the noise level shown in the difference spectra here is only about 0.2 mOD from all contributions. We did not use any other baseline correction other than solvent (D_2O, HOD) and vapor subtractions when necessary.

Transient IR spectroscopy. The IR T-jump spectrometer has been previously described[24] and was used with an increased path length (200−300 μm) to extend the time resolution to the 10 ms range.

RESULTS

Despite substantial spectral crowding present in IR protein spectra, the vibrational frequencies of specific bonds within a protein complex are assigned by performing sensitive IR difference spectroscopy coupled with isotope-editing procedures. Our procedures, which have not been reported previously in detail, are elaborated in the Materials and Methods section and below.

Figure 1, the FTIR spectra of the LDH/NADH binary and LDH/NADH/oxamate ternary complexes and their difference spectra, calibrates the subtraction fidelity available to our instruments and demonstrates the need for isotope editing. The difference spectrum between the ternary and binary complexes

shown as C contains bands whose intensities are about 50 mOD, at least 10 times more intense than those from the expected bound ligand bands (e.g., see Figure 2). Spectrum D is a control and was obtained under conditions where both positions of the sample shuttle were occupied by the same LDH/NADH/oxamate sample; hence, it should yield a null spectrum. To the extent that it does not, the difference spectrum determines the level of incomplete subtraction fidelity of the difference spectrometer. The evident ±0.2 mOD incomplete subtraction fidelity is sufficient for the determination of even very weak bands, as shown below. The results shown in Figure 1 suggest that, in the isotope-edited difference FTIR studies of proteins, the focus should be on the reduction of "artifacts" caused by unmatched protein/ligand concentration ratios of the two samples and/or slightly unbalanced optical paths between the two samples. We adopt a systematic approach, as described in the Materials and Methods, to reduce such protein "artifacts" iteratively such that bands are assigned with confidence.

Although we failed to observe the bound oxamate spectrum in Figure 1C, there are several useful observations can be made from these results. One is that longer signal averaging will not improve our signal-to-noise because the shot noise level is already significantly lower than the expected intensity of bands from the bound ligand. The other is that the binding of oxamate to LDH/NADH affects the structure sensitive amide-I′ (the prime denotes that the amide protons are deuterated). It is clear that binding produces a number of structural changes within the protein, with concomitant spectral features, likely involving at least the protein's hydrogen bonding network.

Isotope-Edited Difference Spectra. To obtain the IR spectrum of bound oxamate, [^{13}C]oxamate was prepared in anticipation of performing isotope editing studies. Figure 2 shows the difference spectra between solutions of LDH/NADH/[$^{12}C_1$]oxamate and LDH/NAD/[$^{13}C_1$]oxamate. Since the two protein solutions are taken independently from each other, there is always some misbalance between the two parent protein spectra affecting, mostly, relative signal size from the protein and background water. Correct identification of bands resulting from the editing apart from protein background is obtained by varying the subtraction factor iteratively (see ref 17). Before subtraction, the intensities of the two spectra are normalized so that the subtraction factor is close to one. In Figure 2, the top curve shows the slightly undersubtracted difference spectrum while the bottom curve shows the slightly oversubtracted one with respect to the major IR protein bands at, e.g., 1646 cm^{-1} (the band at 1455 cm^{-1} is a HOD water bending band; subtractions of this water band can be handled separately, if needed). The vibrational bands related to oxamate C_1 motions appear as positive−negative pairs. They do not change their intensities substantially or disappear with the variation of the subtraction factor, as demonstrated for 1581/1569 and 1646/1611 cm^{-1} pairs. In addition, their positions in all iterations were very reproducible, well within 0.5 cm^{-1}, at least for the three sharp bands at 1581, 1569, and 1646 cm^{-1}. On the other hand, the protein bands in the difference spectra, arising from a (small) mismatch between the two samples, generally significantly change their appearance (frequency and/or intensity) as the subtraction factor is varied.

It should be noted that the "correct" subtraction factor may not be the same for the entire spectral region due to the well-known baseline problem often confronted in IR spectroscopy. For example, the bottom curve in Figure 2 may be more appropriate for the spectral region below 1600 cm^{-1}, including the 1581/1569 cm^{-1} pair, because the baseline in that region is well-defined and the "noise level" is on the order of 0.2 mOD, compatible with the noise level observed in the control experiment shown in Figure 1. Since the signal size of the 1581/1569 cm^{-1} positive/negative pair is more than 1 mOD (5 times higher than the noise level) and their appearances and intensity levels did not change in the later subtraction iterations, they are confidently assigned to signals from bound oxamate. On the other hand, the data in Figure 2 shows that the subtraction factor above 1600 cm^{-1} should be ~1% less since, in the bottom curve, the "artifact" band at 1659 cm^{-1} becomes too pronounced. This band is apparently a component of the 1659 cm^{-1} band found in the difference spectrum between the ternary and binary complex shown in Figure 1C. In some cases, these bands, clearly not from the bound ligand, can be assigned with additional measurements. For example, the 1455 cm^{-1} band can be assigned to the HOD bending mode, due to the small imbalance of the hydrogen concentration between the two deuterated samples. However, many of these bands remain unassigned, for example, the 1659 cm^{-1} band, and may be artifacts of the subtraction process. Since these bands normally do not appear as isotope pairs in the difference spectrum, they may be excluded in the analysis. In general the most convincing assignments can be made for positive-negative pairs that show an expected isotope shift, such as the 1646/1611 cm^{-1} pair. The appearance of the 1581/1569 cm^{-1} pair was totally unexpected and shows only a small isotope effect; additional measurements described below were conducted to confirm that this difference pair is associated with the bound ligand.

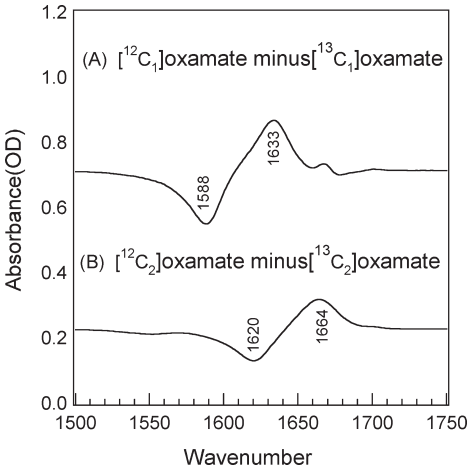

Figure 3. Difference FTIR spectra between (A) [$^{12}C_1$]oxamate and [$^{13}C_1$]oxamate in solution and (B) [$^{12}C_2$]oxamate and [$^{13}C_2$]oxamate in solution. Samples were prepared in D_2O with a concentration of 100 mM.

Figure 3 shows the ^{13}C isotope edited difference FTIR spectra of oxamate in solution with ^{13}C labels at C_1 (panel A) and C_2 (panel B). For the oxamate carboxyl group, the two C···O stretches are coupled to form a symmetric stretch at 1350 cm^{-1} (data not shown) and an asymmetric stretch at 1633 cm^{-1}, as identified in the difference spectrum of Figure 3A. The oxamate amide C_2═O stretch mode is found at 1664 cm^{-1}, as identified in the in the difference spectrum of Figure 3B. The ^{13}C-induced shifts of these two modes are 45 and 44 cm^{-1} for $^{13}C_1$ and $^{13}C_2$ labels, respectively.

Figure 4A shows the difference spectrum between LDH/NADH/[$^{12}C_1$]oxamate and the complex with [$^{13}C_1$]oxamate. In

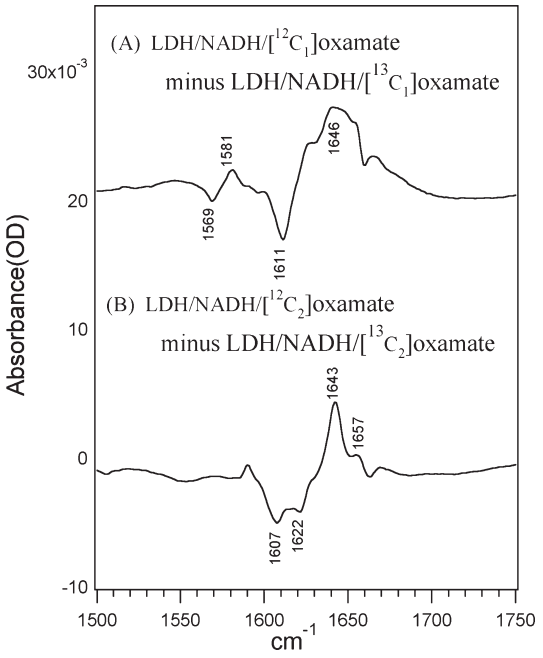

Figure 4. Difference FTIR spectra between (A) LDH/NADH/[$^{12}C_1$]oxamate and LDH/NADH/[$^{13}C_1$]oxamate and (B) LDH/NADH/[$^{12}C_2$]oxamate and LDH/NADH/[$^{13}C_2$]oxamate. See Figure 1 for sample conditions. The reported frequencies are the average of more than five separate measurements as described in the text. The band positions are accurate to within $+1$ cm^{-1}, except for the broad band at 1646 cm^{-1}, which is broadened by mode coupling as discussed in the text.

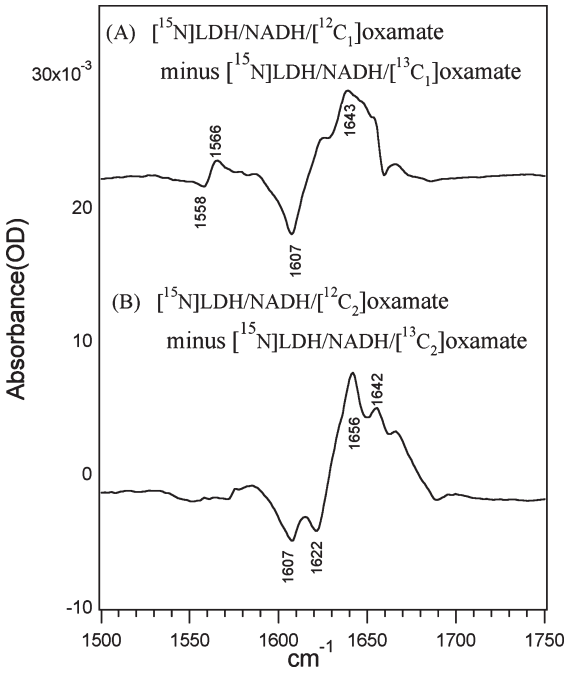

Figure 5. Difference FTIR spectra between (A) LDH/NADH/[$^{12}C_1$]oxamate and LDH/NADH/[$^{13}C_1$]oxamate and (B) LDH/NADH/[$^{12}C_2$]oxamate and LDH/NADH/[$^{13}C_2$]oxamate with uniformly ^{15}N-labeled LDH. See Figure 1 for sample conditions. The reported frequencies are the average of more than five separate measurements as described in the text. The band positions are accurate to within ± 1 cm^{-1} except for the broad band at 1643 cm^{-1}, which is broadened by mode coupling as discussed in the text.

this spectrum, more than one IR band shows a ^{13}C isotope shift, suggesting that the carboxyl asymmetric stretch motion is distributed. The major band centered around 1646 cm^{-1} associated with unlabeled oxamate is quite broad and contains multiple features but becomes sharp at 1611 cm^{-1} upon $^{13}C_1$ labeling. One explanation is that, in the LDH/NADH/oxamate complex, the carboxyl asymmetric stretch is coupled with motions of other portions of oxamate, and this coupling is removed by $^{13}C_1$ labeling. This suggestion is supported by ab initio calculations (see below). Since these bands have similar intensities compared to their solution counterparts and the isotope shifts due to $^{13}C_1$ labeling are $\sim$35 cm^{-1}, only somewhat smaller than the solution value, they can be assigned to the carboxyl asymmetric stretch mode. It is interesting to note that the frequency of the asymmetric stretch mode of the oxamate carboxyl group shifts up by 23 cm^{-1} upon oxamate binding (from 1588 to 1611 cm^{-1} for $^{13}C_1$ labeled bands); such upward shifts can result from stronger hydrogen bonding.[25] The additional minor differential feature at 1581/1569 cm^{-1} is also observed in this difference spectrum. Since the ^{13}C isotope shift here is only 12 cm^{-1}, it can not be assigned to the carboxyl asymmetric stretch even though it must contain atomic motions associated with C_1 to show the (relatively small) ^{13}C shift.

Figure 4B shows the difference spectrum between LDH/NADH/oxamate complex and the complex with [$^{13}C_2$]oxamate. Two IR bands at 1643 and 1657 cm^{-1} shift down by 36 and 35 cm^{-1}, respectively, to 1607 and 1622 cm^{-1} upon $^{13}C_2$ labeling. The simplest interpretation for this result is that the LDH/NADH/oxamate complex consists of two populations, a major component (characterized by a $^{13}C_2$=O bond vibrating at 1607 cm^{-1}) and a minor component (1622 cm^{-1}). Since the C_2=O stretch frequency of the major oxamate component is 21 cm^{-1} lower than that in solution (comparing Figure 3B and Figure 4B), the hydrogen bonding to C_2=O within the protein is stronger than that found in solution, consistent with a structure of a polarized bond predicted to be along the reaction path toward the transition state for this protein (see ref 14). The frequency of the C_2=O stretch of the minor species, on the other hand, is not much different from the solution value (especially when the $^{13}C_2$=O stretches are compared). Similar findings have also been observed in the studies of the LDH/NADH/oxamate complex using phLDH.[20] These results can be correlated to the results from previous Raman difference studies of the NADH C_4–D stretch mode of this ternary complex, where NADH is also found to exist as a major and minor species.[13]

Figure 5A,B shows the isotope-edited difference spectra as in Figure 4A,B except here uniformly ^{15}N-labeled LDH has been used. Comparing spectra 4A and 5A, all IR bands show a small downward shift due to the ^{15}N label. For example, the $^{13}C_1$-labeled carboxyl asymmetric stretch mode at 1611 cm^{-1} in 4A shifts down by 5 cm^{-1} to 1607 cm^{-1} in 5A. Given that the guanidinium moiety of Arg171 is tightly packed against the carboxyl group of bound oxamate,[7] this is direct evidence that motions of the guanidinium moiety are involved in this mode. The differential feature at 1581/1569 cm^{-1} shifts down by 15/11 cm^{-1} to 1566/1558 cm^{-1}, indicating even greater involvement of the guanidinium motion. In clear contrast, the C_2=O stretch modes do not show significant shift upon uniform ^{15}N labeling of the protein (Figures 4B and 5B; bands at 1607 and 1622 cm^{-1} in

Scheme 2. Salt Bridge Model Used in Vibrational Mode Calculations[a]

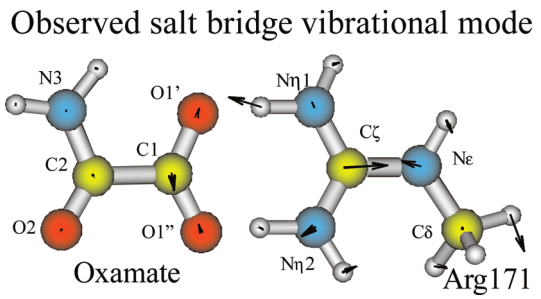

[a] The calculated eigenvector associated with the FTIR detected salt-bridge vibrational mode is also shown.

Figure 5B), even though the oxamate C_2═O bond is strongly hydrogen bonded to two LDH NH groups from Arg109 and His195 (see Scheme 1). Thus, just strong hydrogen bonding alone, even with ionic nature (since both Arg109 and His195 are likely charged), is not sufficient to cause vibrational coupling between C_2═O and its hydrogen bond partner. All together, our experimental results firmly established that the derivative feature at 1581/1569 cm^{-1} in 4A must be due to a vibrational mode that involves the motions from both sides of the carboxyl-guanidinium salt bridge. Surprisingly, the "salt bridge" IR band is quite narrow. This shows that even though it consists of motions of atoms lying on both the carboxyl and guanidinium fragments, which are not covalently bonded, the inhomogeneous line broadening, normally observed in such cases, is not present here. All this indicates the strong bond formed by ionic interactions between oxamate and Arg171 is very uniform, with virtually no conformational flexibility.

The newly assigned salt bridge mode is not limited to the oxamate bound to bsLDH but appears to be a general feature of LDH-bound pyruvate-like substrates. A similar mode was also observed, but not assigned, in the bsLDH/NAD-pyruvate adduct[26] as well as for oxamate bound to phLDH.[21] It seems likely that the frequency of this mode may be used to estimate the strength of the salt bridge. For example, it appears at 1589/1582 cm^{-1} in the phLDH ternary complex,[21] significantly different from the 1581/1569 cm^{-1} frequencies observed here in bsLDH. The measured dissociation constants for oxamate in these two LDH ternary complexes differ by a factor of 10, suggesting a possible correlation between the strength of the salt bridge and its vibrational mode frequency. However, further studies are required to confirm this suggestion.

Normal Mode Analysis. A normal-mode analysis was performed in order to (1) find an explanation for the observed broadness of the asymmetric stretch mode in the LDH/NADH/oxamate complex (the positive band at 1646 cm^{-1} in Figure 4A) relative to the much sharper corresponding band with $^{13}C_1$ labeling (the negative band at 1611 cm^{-1}) and (2) characterize the carboxyl-guanidinium salt bridge mode at 1581/1569 cm^{-1} (Figure 4A). We also probed how hydrogen bonding or salt bridge formation affects the frequency of the deprotonated carboxyl antisymmetric stretch mode. In our normal-mode analysis, three models are used: isolated oxamate, oxamate with two water molecules hydrogen bonded to its carboxyl group, and the oxamate−methyl guanidinium complex shown in Scheme 2. In the oxamate−water complex, the two water molecules are at positions similar to those of the two Nη atoms of the guanidinium group in LDH.

In our calculations, the electronic structures of the model systems were optimized at the B3LYP/6-31g** level as implemented in Guassian 98,[27] and the vibrational frequencies were then calculated at the same level. Before discussing the calculated frequency quantitatively, it is necessary to point out that the observed stretch frequencies are normally overestimated by the calculations, typically uniformally by 5−15%. Here we do not use scaling factors to come to precise quantitative agreement but base the assignments on calculated spectral shifts that are within the 5−15% error of the calculations.

Effect of Hydrogen Bonding to the COO^- Asymmetric Stretch Frequency. The calculated modes that contain significant oxamate asymmetric C···O stretch motion in these model compounds are listed in Table 1. The stretch motions of the two C···O bonds of a $-COO^-$ moiety are normally coupled to form one symmetric (υ_s) and one asymmetric (υ_a) stretch pair. In isolated oxamate, this asymmetric $-C_1OO^-$ stretch is also coupled with the C_2═O stretch due to their similar frequencies. When the oxamate carboxyl group is hydrogen bonded to two water molecules, the asymmetric $-C_1OO^-$ frequency is no longer coupled to the C_2═O stretch and shifts down by 21 cm^{-1} (see Table 1), as we would expect since hydrogen bonding should weaken the two C···O bonds and thereby lower their stretch frequencies.

Effect of Salt Bridge Formation on the $-COO^-$ Asymmetric Stretch Frequency. As shown in Table 1, the results of normal mode calculations on isolated oxamate and its complex with a guanidinium group shows that salt bridge formation *increases* the $-C_1OO^-$ asymmetric stretch (compare 1808 and 1820 cm^{-1} modes in the salt bridge with 1771 and 1778 cm^{-1} modes in the isolated oxamate). This is somewhat unexpected since the interaction on the C···O bonds is stronger in the salt bridge than in solution, and, for a simple C═O bond, stronger interactions almost always result in a longer C═O bond and lower stretch frequency. Although our calculations predict longer average C···O bonds in the salt bridge, its asymmetric stretch frequency is nevertheless higher. It is likely the ring structure of the salt bridge puts a significant constraint on the carboxyl group motion to cause its upward frequency shift. Furthermore, the $-C_1OO^-$ asymmetric stretch motion is coupled to the C_2═O stretch to form two delocalized modes. However, the coupling is removed upon $^{13}C_1$ labeling, and only one mode contains asymmetric stretch character.

On the basis of these results, it is reasonable to conclude that the relatively large blue shift of the oxamate $-C_1OO-$ asymmetric stretch mode upon its binding to the LDH/NADH complex is caused by the salt bridge formation. In addition, the broad band at 1646 cm^{-1} in Figure 4A, which is sensitive to the $^{13}C_1$ labeling, is likely due to mode mixing between asymmetric $-C_1OO^-$ and C_2═O stretches. Since there are more than one C_2═O stretch modes as indicated in Figure 4B, possible couplings between $-C_1OO^-$ asymmetric and C_2═O stretches cause the broadness of the $-C_1OO^-$ asymmetric band in the LDH/NADH/oxamate complex. Upon $^{13}C_1$ labeling, the $^{13}C_1OO^-$ asymmetric stretch mode becomes homogeneous and shows up as a sharp band at 1611 cm^{-1} in Figure 4A.

Characterization of the Salt Bridge Mode. The results of calculations for the salt bridge complex show that besides "normal" $-C_1OO^-$ asymmetric modes whose motions are more or less isolated to the deprotonated carboxyl group, the observed 1597 cm^{-1} mode also contains significant -C_1OO^- asymmetric stretch character. This mode involves an out-of-phase combination

Table 1. Experimentally Observed and Calculated Vibrational Modes with Oxamate Carboxyl Asymmetric Stretch Character[a]

				calculated eigenvectors									
complex		calculated		oxamate bonds					Arg171 bonds				
isotope labels	exp	modes	freq	$C_1-O_{1'}$	$C_1-O_{1''}$	C_2-C_1	$C_2=O$	C_2-N_3	$C\zeta-N\eta1$	$C\zeta-N\eta2$	$C\zeta-N\varepsilon$	$N\varepsilon-C\delta$	D
oxamate		υ_a	1771	1.22	−0.73	0.25	−0.25	0.14					
		$C_2=O$	1778	0.25	−0.17	−0.4	1.31	−0.26					
oxamate +2 D_2O		υ_a	1750 (−21)	1.22	−0.72	0.14							
ND (salt bridge)	1581		1597	0.24	−0.28				0.32	0.51	−0.73	0.2	0.42
	1640*	υ_a, $C_2=O$	1808	−0.35	0.47	−0.24	0.64	−0.26		0.23			
	1655*	υ_a, $C_2=O$	1820	0.38	−0.4		0.75	−0.29					
+$^{13}C_1$ (salt bridge)	1569 (−12)		1592 (−5)	0.2	−0.24				0.36	0.46	−0.74	0.2	
	1611 (−37*)	υ_a	1789 (−25*)	−0.36	0.46		0.16			0.26			
+$^{15}N(E)$ (salt bridge)	1566 (−15)		1582 (−15)	0.21	−0.25				0.31	0.50	−0.7	0.16	0.41
	1640*	υ_a, $C_2=O$	1803	−0.4	0.52		0.38	−0.16		0.21			
	1655*	υ_a, $C_2=O$	1818	0.3	−0.29		1.02	−0.34					
+$^{15}N(E)$ +$^{13}C_1$ (salt bridge)	1558 (−8)		1578 (−4)	0.18	−0.22				0.35	0.45	−0.71	0.16	
	1607 (−40*)	υ_a	1780 (−31*)	−0.36	0.47					0.22			

[a] Exp: experimentally observed frequencies; oxamate: isolated oxamate; oxamate +2 D_2O: oxamate complexed with two water molecules hydrogen bonded to the carboxyl group of the oxamate at positions similar to those of the two Nη atoms of the guanidinium (see Scheme 2). The numbers in the parentheses are relative shifts compared to those from isolated oxamate; ND: LDH/NADH/oxamate sample was in D_2O or all NHs in the model were replaced with NDs when the frequencies were calculated. *: The observed asymmetric bands appear as a broad feature between 1640 cm^{-1} and 1655 cm^{-1}. +$^{13}C_1$: in addition to ND, C_1 of oxamate was labeled with ^{13}C. The numbers in the parentheses are relative shifts compared to those from ND. +$^{15}N(E)$: in addition to ND, LDH is uniformly labeled with ^{15}N. The numbers in the parentheses are relative shifts compared to those from ND. +$^{15}N(E)$+ $^{13}C_1$: in addition to ND, LDH is uniformly labeled with ^{15}N and C_1 of oxamate was labeled with ^{13}C. The numbers in the parentheses are relative shifts compared to those from +$^{15}N(E)$.

of the guanidinium $C_\zeta-N_\eta$ and $C_\zeta-N_\varepsilon$stretch motions; the calculated isotope shift upon $^{13}C_1$ and uniform ^{15}N labeling of the guanidinium group are −5 $cm^{-1}$and 15 cm^{-1}, respectively (see Table 1). Although the calculated $^{13}C_1$ isotope shift is (−5 cm^{-1}) significantly smaller than the observed −12 cm^{-1} shift of the 1581 cm^{-1} band (Figure 4A), the observed frequency shift is derived from a difference spectrum where the difference between the two peak frequencies are likely smaller than their band widths (typically >15 cm^{-1}); in such a case, the apparent frequency difference is larger than their real frequency difference.[17] Furthermore, the calculated ^{15}N shift (15 cm^{-1}, see Table 1) of this mode is in very good agreement with the ^{15}N shift of the 1581 cm^{-1} band (15 cm^{-1}, compare Figure 4A and 5A). On the basis of these results, the assignment of the 1581 cm^{-1} band in the difference FTIR spectrum (Figure 4A) to a delocalized vibrational mode involving stretch motions from both sides of the carboxyl−Arg salt bridge is firmly established by both experimental results and theoretical vibrational analysis.

Interconversion Dynamics between the 'Major' and 'Minor' Protein Complex Species. As shown above, the Michaelis mimic complex, LDH/NADH/oxamate, contains two populated conformations: one characterized by oxamate $^{13}C_2$ stretch bands at 1607 (major populated conformation and closer to the transition state of the on-enzyme catalyzed event) and 1622 cm^{-1} (minor population, further from the transition state). If these two conformers thermally interconvert on a time scale as fast or faster than the overall catalytic rate (around a millisecond for LDH), then the kinetic scheme, and resultant thermodynamics, of the on-enzyme reaction pathway of substrate to product requires their explicit incorporation. The population of these two conformers is temperature dependent as shown by the temperature-dependent static isotope-edited IR spectra (Figure 6, inset). Hence, temperature jump relaxation

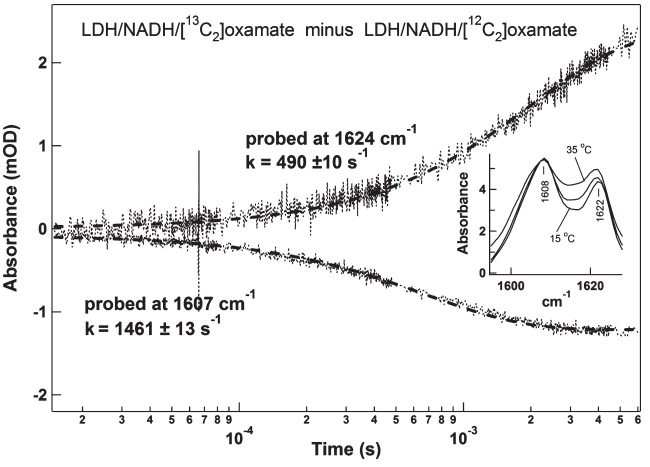

Figure 6. Kinetic isotope-edited IR difference T-jump spectra for wild-type bsLDH probed at 1607 cm^{-1} (upper trace) and 1624 cm^{-1} (lower trace). The difference T-jump traces were obtained by subtracting the LDH/NADH/[$^{12}C_2$]oxamate trace from that of the LDH/NADH/[$^{13}C_2$]oxamate for the kinetic traces. The temperature-dependent static isotope-edited IR spectra are shown in the inset. The IR spectra at different temperatures represent LDH/NADH/[$^{13}C_2$]oxamate minus LDH/NADH/[$^{12}C_2$]oxamate. Ternary complexes were formed by mixing 0.6 mM LDH, 0.6 mM NADH, and 0.6 mM oxamate in 0.1 M triethanolamine (TEA) at pH = 6.

spectroscopy can probe the interconversion kinetics of the two species. Isotope-edited IR difference T-jump spectra probed at 1607 cm^{-1} (upper trace) and 1624 cm^{-1} (lower trace) are shown in Figure 6. These T-jump traces are conceptually formed in the same way as the static isotope edited FTIR studies. After the sample's temperature is suddenly raised, the time-dependent IR

absorbance at specific frequencies of LDH/NADH/[$^{12}C_2$]-oxamate and LDH/NADH/[$^{13}C_2$]oxamate are measured and subsequently subtracted, leaving a time-dependent difference spectrum containing only IR signatures affected by the label.[21,24] As can be observed, the concentration of the minor species (as measured at 1624 cm^{-1}) increases while the major conformer (1607 cm^{-1}) decreases. The two conformers interconvert on the submillisecond time scale, although not directly since the observed relaxation times differ. We have shown previously that such kinetic behavior can be understood via a kinetic model that has the pathway of interconversion occurring between a common intermediate.[21]

DISCUSSION AND CONCLUSION

The primary goal of this study is to explore the energy landscape of the Michaelis complex of LDH with probes of structure at atomic resolution. From general notions of the structures of proteins, the Michaelis complex of the enzyme certainly consists of an ensemble of conformations, interconverting on various time scales from picoseconds to minutes. Interconversions amongst most members of the ensemble have little or no bearing on the mechanism of catalysis. We are interested here in characterizing those that are relevant to the reaction coordinate; in general, this has been very difficult to accomplish experimentally. The vibrational studies herein are able to isolate and characterize at least some portions of the relevant energy landscape.

Two specific questions come to mind. To what extent has the conformational degrees of freedom available to the interacting substrates (here NADH and pyruvate) in solution collapsed upon binding to the enzyme? And, does the observed spectrum of these conformations exhibit varying degrees of "closeness" to the transition state of the on-enzyme chemical reaction? We have some excellent "fine scale" spectroscopic markers of protein states available for the LDH system to answer these questions, at least in part. For the LDH/NADH/pyruvate ternary complex, the vibrational bands associated with the C_2═O stretch and the antisymmetric $-COO^-$ stretch of bound substrate and the C_4−H stretch of bound NADH are easily determined by isotope-edited Raman or IR studies. Moreover, we discovered in the course of our study a very unusual and useful diagnostic "salt-bridge" mode formed by the salt bridge between the carboxyl group of bound substrate and a protein Arg group.

The molecular basis of LDH activity has been extensively studied. Stabilization of the polar transition state is responsible for about half of the enzyme's activity; this factor is easily assessed by the change in frequency (bond polarization) of the substrate (pyruvate) C_2═O stretch.[14] Some rate enhancement comes about from ring deformation of the nicotinamide group of NADH; this is assessed by studies of the C_4−H stretch,[13] and most of the remaining enzyme-induced rate comes about by bringing the NADH and pyruvate substrates in close proximity and alignment. In this study, we have employed the substrate mimic oxamate to avoid any complications of on-enzyme chemistry; this molecule has been shown in many previous studies to be an excellent mimic of LDH's substrate pyruvate.

There clearly has been a substantial reduction in the number of states available to the substrates pyruvate (as modeled by the substrate mimic, oxamate) and NADH when bound to LDH relative to when in solution. The C_2═O line width(s) of the critical C═O bond vibration of the bound oxamate are substantially smaller than the solution counterparts (compare Figures 3B and 4B). The broad line width observed for oxamate in solution is due to heterogeneous broadening (multiple conformations with a range of vibrational frequencies) and so the reduction of bandwidth is a direct, if qualitative, indication of a restricted set of conformations. We have previously found the same for the C_4−H stretch mode of bound NADH.[13]

However, not all dynamics have been frozen out. The isotope-edited IR difference studies show that there are two forms of the bound inhibitor: a major form in which the hydrogen bonding interactions with the oxygen of the C_2═O moiety is significantly stronger than that in solution, and a minor form, about half as populated, in which the hydrogen bonding with C_2═O is similar to that found in solution. In previous isotope-edited Raman studies of this same complex,[13,28] it was found that the bound reduced nicotinamide ring adopts a "half-boat" conformation. Furthermore, two conformations were found, also populated in a 2/1 concentration ratio. In the major form, the estimated angle of the C_4 ring carbon with respect to the other carbon atoms is around 10−15°, with the pro-R hydrogen (A side) in a pseudoaxial geometry and the pro-S hydrogen (B side) pseudoequatorial. In the minor form, the out-of-plane distortion of the C_4 carbon is somewhat less, and the pro-S hydrogen (B side) adopts a pseudoaxial geometry while the pro-R hydrogen (A side) is pseudoequatorial. In both conformations, the carboxylate group appears to be "locked into place", forming the strong salt bridge with Arg171. In previous kinetic studies on phLDH[21] and the current study here on bsLDH, these two forms interconvert on the submillisecond time scale.

The more populated conformation is poised for catalysis since (1) its ring structure is consistent with the transition state structure of the hydride transfer reaction predicted by theoretical calculations[10−12] and (2) the polarization of the substrate C_2═O bond found in the major conformation is a crucial molecular factor in the catalytic power of LDH (see Introduction in ref 14). Overall, the major populated structure of the LDH/NADH/oxamate complex represents an advanced stage of the true substrate LDH/NADH/pyruvate complex along the enzyme-catalyzed reaction path. In contrast, the minor populated conformation of the LDH/NADH/oxamate complex does not resemble one that is catalytically competent. The NADH ring puckering is toward the other face of the nicotinamide, forcing the pro-R hydrogen into a pseudoequatorial position, a wrong position for putative hydride transfer, and, perhaps even more importantly, the hydrogen bonding strength to C_2═O is decreased substantially (even weaker than that in solution, possibly because the ring conformation forces an increase of the volume of the active site cavity). We can not calculate the difference in catalytic rates between the two conformers, but, based on studies of the structural basis for the reactivity as catalyzed by LDH, the two structures would at least exhibit several (as many as 8) orders of magnitude ratio in relative rate enhancement.[9,14]

We suspect that there is some conformational "complexity" for the Michaelis complex with regards to the distance and alignment of the two interacting substrates as well. The dynamical nature of the protein-bound so-called NAD−pyruvate adduct is entirely different from that for either oxamate or pyruvate-bound LDH.[26] The simple change of a covalent bond between NADH's C_4 and pyruvate's C_2 (hence imposing a close and precise alignment of the two reacting molecules) essentially "freezes" the protein complex. Only a single polarized C_2═O species is observed, and there are no observed submillisecond motions at the active site even up to temperatures near the melting

point of the protein. Clearly the dynamical nature of the Michaelis complex and the LDH/NAD−pruvate adduct are quite different, strongly suggesting that the enzyme-bound NADH−pyruvate distance experiences a distribution of distances. Moreover, calculations of the donor−acceptor distance within the Michaelis complex of LDH shows that, of the many conformations available to the protein, only a small subset are competent.[5,6]

The present experiments then have identified, and structurally characterized, at least two distinct conformers of the ternary complex mimic the Michaelis complex of LDH. These two states are both substantially populated, meaning that the overall Gibbs free energies of the protein complex are virtually the same. On the other hand, from previous work relating catalytic activity to active site structure, one of the conformers is active while the other represents a very inactive structure. Since the two species are interconverting[21] on a time scale faster than the observed k_{cat} for this enzyme (a few milliseconds), catalytic efficiency is impaired by about a factor of 2 based on just these two structures. We have examined the temperature dependence of the populations of the two conformers by determining the temperature dependence of the two vibrational bands. The errors in the measurement are significant due to the small intrinsic signal size versus background signals. However, an approximately 10% change is observed over a 10 °C interval, suggesting a 1.7 kcal/mol enthalpy. Typical transition state barriers (Gibbs free energy) to catalysis, in the usual Eyring treatment, are around 13 kcal/mol given a ca. 1 ms transition time. Hence, the data here suggests that the measured thermodynamics of substrate−product interconversion for LDH is affected by the ensemble nature of the Michaelis complex. The measured enthalpies and free energies of k_{cat} include ground state effects. Such findings are commonplace for enzyme systems whose reaction pathways are relatively complicated, involving a couple or more intermediates well separated in time. The LDH system, by contrast, involves a catalytic system where all chemical steps (proton and hydride transfer) occur concertedly, or nearly so, on the subpicosecond time scale, as suggested in recent computational studies.[12]

We have supposed that enzyme-catalyzed chemical catalysis is an inherently dynamical process in that the enzyme substrate system does a stochastic search through all the available configuration space until all atomic coordinates and momenta are in place to carry the system from substrate side to product side. The configuration space available to such a search is, of course, limited by the structure of the Michaelis complex so that the enzyme "finds" the reaction coordinate in milliseconds. This point is to be emphasized. The "stochastic search" does not imply a search through all possible states; this space is so large that this hunt would take a very long time indeed. On the other hand, what we have shown here is that the hunt through available configurations in the LDH system includes atomic arrangements that occupy a relatively stable energy basin which are inactive with regard to catalysis. The reaction pathway from binding to chemical step involves interconverting of these states to search for reactive configurations.

AUTHOR INFORMATION

Corresponding Author

*Address: Department of Biochemistry, Albert Einstein College of Medicine, Bronx, New York 10461, United States. Phone: 718-430-3024. Fax: 718-430-8565. E-mail: call@aecom.yu.edu.

ACKNOWLEDGMENT

This work was supported by the Institute of General Medicine of the National Institutes of Health, program project grant number 5P01GM068036 and by the National Institute of Biomedical Imaging and Bioengineering grant EB001958.

REFERENCES

(1) Austin, R. H.; Beeson, K. W.; Eisenstein, L.; Frauenfelder, H.; Gunsalus, I. C. *Biochemistry* **1975**, *14*, 5355.
(2) McCammon, J. A.; Gelin, B. R.; Karplus, M. *Nature* **1977**, *267*, 585.
(3) Frauenfelder, H.; Sligar, S. G.; Wolynes, P. G. *Science* **1991**, *254*, 1598.
(4) Frauenfelder, H.; McMahon, B. H.; Fenimore, P. W. *Proc. Natl. Acad. Sci. U.S.A.* **2003**, *100*, 8615.
(5) Pineda, E. T.; Schwartz, S. D. *Philos. Trans. R. Soc.* **2006**, *361*, 1433.
(6) Pineda, J. R. E. T.; Antoniou, D.; Schwartz, S. D. *J. Phys. Chem. B* **2011**, *114*, 15985.
(7) Wigley, D. B.; Gamblin, S. J.; Turkenburg, J. P.; Dodson, E. J.; Piontek, K.; Muirhead, H.; Holbrook, J. J. *J. Mol. Biol.* **1992**, *223*, 317.
(8) Wigley, D. B.; Muirhead, H.; Gamblin, S. J.; Holbrook, J. J. *J. Mol. Biol.* **1988**, *204*, 1041.
(9) Burgner, J. W.; Ray, W. J. *Biochemistry* **1984**, *23*, 3636.
(10) Wu, Y. D.; Houk, K. N. *J. Org. Chem.* **1993**, *58*, 2043.
(11) Almarsson, O.; Bruice, T. C. *J. Am. Chem. Soc.* **1993**, *115*, 2125.
(12) Basner, J. E.; Schwartz, S. D. *J. Am. Chem. Soc.* **2005**, *127*, 13822.
(13) Chen, Y.-Q.; van Beek, J.; Deng, H.; Burgner, J.; Callender, R. *J. Phys. Chem.* **2002**, *106*, 10733.
(14) Deng, H.; Zheng, J.; Clarke, A.; Holbrook, J. J.; Callender, R.; Burgner, J. W. *Biochemistry* **1994**, *33*, 2297.
(15) Braiman, M. S.; Rothschild, K. J. *Annu. Rev. Biophys. Biophys. Chem.* **1988**, *17*, 541.
(16) Cheng, H.; Sukal, S.; Deng, H.; Leyh, T. S.; Callender, R. *Biochemistry* **2001**, *40*, 4035.
(17) Callender, R.; Deng, H. *Annu. Rev. Biophys. Biomol. Struct.* **1994**, *23*, 215.
(18) Liu, A.; Hu, W.; Majumdar, A.; Rosen, M. K.; Patel, D. J. *J. Biomol. NMR* **2000**, *17*, 305.
(19) Birdsall, B.; Polshakov, V. I.; Feeney, J. *Biochemistry* **2000**, *39*, 9819.
(20) McClendon, S.; Vu, D.; Clinch, K.; Callender, R.; Dyer, R. B. *Biophys. J.* **2005**, *89*, L07.
(21) Deng, H.; Brewer, S. H.; Vu, D. V.; Clinch, K.; Callender, R.; Dyer, R. B. *Biophys. J.* **2008**, *95*, 804.
(22) Zhadin, N.; Gulotta, M.; Callender, R. *Biophys. J.* **2008**, *95*, 1974.
(23) White, A. J.; Wharton, C. W. *Biochem. J.* **1990**, *270*, 627.
(24) Callender, R. H.; Dyer, R. B. *Chem. Rev.* **2006**, *106*, 3031.
(25) Gu, Z.; Zambrano, R.; McDermott, A. *J. Am. Chem. Soc.* **1994**, *116*, 6368.
(26) Gulotta, M.; Deng, H.; Deng, H.; Dyer, R. B.; Callender, R. H. *Biochemistry* **2002**, *41*, 3353.
(27) Frisch, M. J.; Trucks, G. W.; Head-Gordon, M.; Gill, P. M. W.; Wong, M. W.; Foresman, J. B.; Johnson, B. G.; Schlegel, H. B.; Robb, M. A.; Replogle, E. S.; Gomperts, R.; Andres, J. L.; Raghavachari; K., J. S., B.; Gonzalez, C.; Martin, R. L.; Fox, D. J.; Defrees, D. J.; Baker, J.; Stewart, J. J. P.; Pople, J. A. Gaussian 98; Gaussian, Inc.: Pittsburgh, PA, 1998.
(28) Deng, H.; Zheng, J.; Sloan, D.; Burgner, J.; Callender, R. *Biochemistry* **1992**, *31*, 5085.